Performance Analysis of Reconfigurable Intelligent Surface-Assisted Wireless Communication Systems under Co-Channel Interference

YUYING BIAN[1], DANDAN DONG[1], JING JIANG[2], MEMBER, IEEE, AND KANG SONG[1,2], MEMBER, IEEE

[1]College of Electronic & Information Engineering, Qingdao University, Qingdao, Shandong 266071, CHINA
[2]Shaanxi Key Laboratory of Information Communication Network and Security, Xi'an University of Posts & Telecommunications, Xi'an, Shaanxi 710121, CHINA

CORRESPONDING AUTHOR: Kang Song (e-mail: sk@qdu.edu.cn).

ABSTRACT Reconfigurable Intelligent Surface (RIS) can intelligently control the wireless propagation environment by adjusting the signal phase and amplitude in real time, which is considered as one of the key technologies of 6G. Although RIS-assisted wireless communication systems greatly improve transmission efficiency under ideal conditions, there are various uncertainties in actual communication systems. In this paper, RIS-assisted communication system is investigated where the RIS cannot completely eliminate the phase error and the user location is randomly distributed with uncertainty. In addition, there are some interference sources around the user, which are simplified as co-channel interference (CCI). Then we study the performance of RIS-assisted communication system, and derive the closed-form expressions for the outage probability (OP) and channel capacity of the system. Furthermore, we analyze the effects of various parameters on the OP and channel capacity. Finally Monte Carlo simulation is carried out which verify the accuracy of the derivation.

INDEX TERMS Reconfigurable intelligent surface, Co-channel interference, Outage probability, Channel capacity.

I. INTRODUCTION

RECONFIGURABLE intelligent surface (RIS), an electromagnetic metasurface consisting of a large collection of low-cost passive reflecting elements [1], [2], which is considered as one of the key technologies for 6G. The typical elements of RIS are meta-atoms, which are usually designed with multiple discrete phase states that can correspond to different electromagnetic correspondences. By controlling the states of the meta-atoms on the meta-surface through software programming, the phase adjustment of the incident signal could be achieved, and various reflecting and scattering profiles can be obtained, enabling intelligent control of the wireless propagation environment without additional energy consumption and extremely promising applications in next-generation mobile communications [3], [4]. One of the significant applications of RIS is the creation of additional line-of-sight (LoS) links between base stations and user devices to increase the achievable data rate of the system [5], [6]. In addition, in 6G networks, RIS can be deployed in large quantities, which can be arranged on the glass of high-rise buildings, vehicles or drones, greatly solving the problem of energy loss due to the presence of obstacles in the communication channel [7]. RIS can also support high wireless channel capacity, effectively expanding the

signal coverage, reducing the size and energy consumption of multi-antenna systems, and mitigating some negative effects of wireless channels, such as multipath fading and Doppler effect [8].

In recent years, studies on numerous aspects of RIS have emerged in academia. As mentioned in [9] and [10], RIS-assisted communication systems are assumed to perfectly eliminate phase errors for the sake of analysis. In [11] the authors propose RIS-assisted medium access control (MAC) protocols for uplink traffic and low-power communication for a large number of users in IoT networks, where RIS configuration parameters can be reserved for each user by introducing a negotiation phase prior to the actual data transmission. However, since it is not possible for RIS to completely eliminate phase errors in practical applications, a number of papers further consider the impact of phase errors on system performance. For example, in [12] the authors analyze the system performance with quantized phase errors and obtain the outage probability (OP) at high signal-to-noise ratio. The authors in [13] derive closed-form expressions for the OP and traversal capacity under real phase shift conditions. On the other hand, the authors in [14], combine RIS with deep learning to propose a new deep reinforcement learning algorithm to optimize the RIS phase shift. In [15] the authors evaluate the performance of RIS-assisted wireless communication systems using an approximation of the achievable data rate and investigate the effect of the finite phase shift of the RIS on the transmitted data rate.

There is also a large body of papers that investigate the impact of the relative position of the RIS with respect to the user and the base station on the communication performance [16], [17]. The authors investigate the effect of the horizontal distance from the RIS to the user on the system performance and find the optimal location of the RIS [18]. In [19] it is assumed that the RIS is randomly distributed on a ring with a fixed radius centered on the base station, where the influence of RIS location on the channel capacity has been investigated. In [20] the authors artificially introduce some controllable paths in RIS-assisted wireless communication systems, which are used to prevent multipath fading and to achieve equalization in the transmission process. Co-channel interference (CCI) is an undesired phenomenon that arises due to the aggressive reuse of frequency channels with high spectrum utilization in wireless communication system [21] and severely degrades the quality of the desired received signal, it is very important to analyse its effects. There is a lot of papers used to study the performance of wireless systems in the presence of CCI [22]–[24]. In [25] the authors investigate the performance of RIS-assisted networks in the presence of destination interference and gives a multi-RIS selection scheme. In [26] the authors investigate the communication between the RIS-assisted UAV and the desired vehicle and the receive vehicle is subjected to interference from multiple jamming vehicles in operation and compares it with the RIS-free communication system.

As mentioned above, although there are many studies on RIS-assisted wireless communication, most of the above mentioned works only consider the effect of phase error, or relative position as an influencing factor on the wireless communication system, and others study the system idealistically, ignoring the CCI in the vicinity of user devices. However, there are many uncertainties in real communication systems [27]–[29], which bring new challenges to study the performance of RIS-assisted systems under a combination of those uncertain influencing factors. Unlike the existing work, we integrate uncertainties such as phase error and user location, and introduce variable CCI around user device. A mathematical framework is proposed to describe the proposed model, and the OP and channel capacity of the system are further analyzed. The main contributions of this paper could be summarized as follows:

- Unlike previous analysis of RIS-assisted ideal wireless systems, the complicated environment around the user device has been introduced into the investigated communication system. The effect of the presence of variable CCI around the user device in the RIS-assisted communication system is considered based on the effect of distance as well as phase error. The analysis of the CCI effectively reflects that the performance of the wireless communication systems is degraded when there is interference outside of user device, which negatively affects the information reception.
- Closed-form expressions of OP and channel capacity for the RIS-assisted communication system with CCI have been derived, which formulate the relationship between system performance and system parameters. These performance expressions provide the design direction for RIS-assisted networks.
- Extensive simulations using Monte Carlo simulation were performed to verify the accuracy of closed-form expressions. The impact of different influencing factors on the system performance is further analyzed, which provides a useful information for the RIS-assisted wireless communication systems.

In this paper we study the performance of the RIS-assisted wireless communication system in terms of OP and channel capacity. In the system model where there are RIS reflecting elements that obey uniformly distributed phase errors, user device D is randomly distributed in the circle and is subject to both CCI and noise. The main structure of this paper is as follows. In Section II the expression for the received signal of user device D in the communication system and signal to interference and noise ratio (SINR) is obtained, and the probability density function (PDF) of the received SINR of user device D is studied. In Section III, closed expressions for OP and channel capacity are further derived based on the PDF expression of SINR obtained in Section II, combined with the system model and the definition of OP and channel capacity. Monte Carlo simulations are
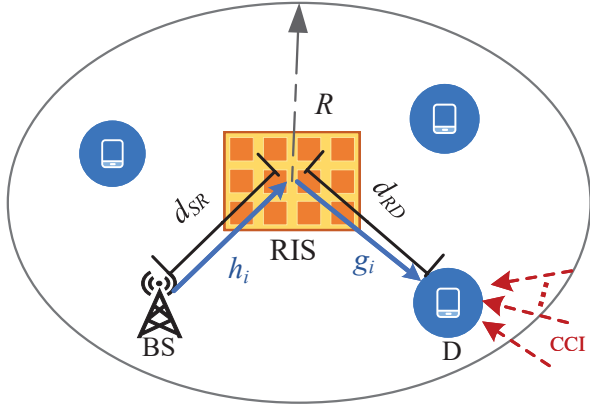
FIGURE 1. system model

performed to verify the derived theoretical results using in Section IV, and the effects of different factors such as transmission distance, path loss exponent, and CCI on the performance of the communication system are analyzed. Finally, the whole paper is summarized and an outlook is given in Section V.

II. SYSTEM MODEL

As shown in Fig. 1, we consider a model of a RIS-assisted communication system consisting of three parts: a base station (BS), a RIS and a user device D, where the RIS contains N reflecting elements. Assume that both BS and the user device are equipped with a single antenna, and there is no direct link from BS to D due to blockage or distance, which means intermediate RIS is needed for the auxiliary communication. In the actual communication system, there is uncertainty in the distance between user device D and RIS, and we assume that user device D is randomly distributed in a circle with R as the coverage radius at the center of RIS. It is assumed that all channels also obey independent Rayleigh fading. Besides signal from BS, user device D could also receive signals from neighbor BS working in the same frequency band, which is treated as CCI. The instantaneous received signal at user device D is the combination of the expectation signal, CCI and Gaussian noise, which can be expressed as

$$y = \sqrt{\frac{P}{d_{SR}^\delta d_{RD}^\delta}} \left[\sum_{i=1}^{N} h_i g_i e^{j\varphi_i} \right] s_{BS} + h_{CCI} s_D + n \quad (1)$$

where s_{BS} is the BS transmit signal, s_D is the D transmit signal, P is the average BS transmit power, δ is the path loss exponent which reflects changes in the wireless communication channel due to possible changes in the RIS communication environment, N is the number of RIS reflecting elements, and d_{SR} and d_{RD} represent the distances from the base station BS to the RIS and the RIS to the user device D respectively, n is the Gaussian white noise generated at D with a mean of zero and the power of

σ_D^2. $e^{j\varphi_i}$ is the adjustable phase generated by the i-th RIS reflecting element. h_i and g_i represent the channel from the BS to the i-th RIS reflecting element and the channel from the i-th RIS reflecting element to the user device D, respectively. $h_i = \alpha_i e^{j\phi_i}$, $g_i = \beta_i e^{j\theta_i}$, they are independent and identically distributed Rayleigh RVs. α_i and β_i represent the amplitude of the channel, while ϕ_i and θ_i represent the corresponding fading channel phase. When D receives information from BS, it suffers from CCI from the same frequency band with the average power of σ^2. Both h_i and g_i obey Rayleigh fading, so h_{CCI} is assumed to be independently Rayleigh distributed with $\mathrm{E}\left[|h_{CCI}|^2\right] = \sigma^2$. To further investigate the other performances of the system, based on equation (1), the instantaneous SINR at D can be obtained as

$$\gamma_D = \frac{\frac{P}{d_{SR}^\delta d_{RD}^\delta} \left| \sum_{i=1}^{N} \alpha_i \beta_i e^{j(\varphi_i - \phi_i - \theta_i)} \right|^2}{|h_{CCI}|^2 + \sigma_D^2} \quad (2)$$

Note that it is hard to estimate the precise channel phase information, although the phases of RIS are designed to eliminate the channel phase, phase errors will be introduced to reflect this effect, which could be denote as ω_i. Generally, ω_i follows the uniform distribution of $(-\pi, \pi)$. Therefore, the instantaneous SINR at D could further be written as

$$\gamma_D = \frac{\frac{\bar{\gamma}}{d_{RD}^\delta} \left| \sum_{i=1}^{N} \alpha_i \beta_i e^{j\omega_i} \right|^2}{|h_{CCI}|^2 + \sigma_D^2} \quad (3)$$

Furthermore, it could rewritten as

$$\gamma_D = \frac{X}{Y + N_0} \quad (4)$$

where $X = \bar{\gamma} X_1$, $X_1 = \frac{X_2}{X_3}$, $X_2 = \left| \sum_{i=1}^{N} \alpha_i \beta_i e^{j\omega_i} \right|^2$, $X_3 = d_{RD}^\delta$, $\bar{\gamma} = \frac{P}{d_{SR}^\delta}$, $Y = |h_{CCI}|^2$, $N_0 = \sigma_D^2$. To facilitate the analysis, we fix the distance from the BS to the RIS and make $d_{SR} = 1$, so $\bar{\gamma}$ is a constant. In general, the power of the CCI is much larger than the noise power, so the noise power can be regarded as a relatively small value.

According to the [30], the PDF of X_2 can be obtained as

$$f_{X_2}(x) = \frac{1}{4\Gamma(N)} G_{0,2}^{2,0} \left(\frac{x}{4} \middle| \begin{matrix} - \\ N-1, 0 \end{matrix} \right) \quad (5)$$

where $G_{p,q}^{m,n} [\bullet]$ is the MeijerG function and $\Gamma(\bullet)$ is the Gamma function.

Based on [30], combined with the distribution of D, we get PDF of d_{RD}

$$f_{d_{RD}}(r) = \frac{2r}{R^2}, 0 \le r \le R \quad (6)$$

where R is the maximum radius that can be covered with the RIS as the center.

Since $X_3 = d_{RD}^\delta$, so it is obvious that the PDF of X_3 is

$$f_{X_3}(x) = \frac{2x^{\frac{2}{\delta}-1}}{\delta R^2}, 0 \le x \le R^\delta \qquad (7)$$

Consequently, according to the relationship among X_1, X_2 and X_3, and $X = \bar{\gamma}X_1$, the PDF of X can be obtained as

$$f_X(x) = \frac{R^{2+\delta}}{2\delta\bar{\gamma}\Gamma(N)R^2}G_{1,3}^{2,1}\left(\frac{R^\delta x}{4\bar{\gamma}}\ \middle|\ \begin{array}{c} -\frac{2}{\delta} \\ N-1, 0, -1-\frac{2}{\delta} \end{array}\right) \qquad (8)$$

Assume that h_{CCI} obeys the Rayleigh distribution and the variance is σ^2. Then the PDF of Y can be expressed as

$$f_Y(y) = \frac{1}{2\sigma^2}e^{-\frac{y}{2\sigma^2}} \qquad (9)$$

Due to the fact that the power of CCI is much larger than that of noise, it is reasonable to omit the noise power in the SINR. Therefore, the PDF at D can be written by combining equation (8) and (9) as equation (10) on the top of the next page, which could be further simplified with the aid of [31]. Therefore, the PDF of γ_D is given by

$$f_{\gamma_D}(\gamma) = \frac{\sigma^2 R^\delta}{\delta\bar{\gamma}\Gamma(N)}G_{2,3}^{2,2}\left(\frac{R^\delta\sigma^2\gamma}{2\bar{\gamma}}\ \middle|\ \begin{array}{c} -1, -\frac{2}{\delta} \\ N-1, 0, -1-\frac{2}{\delta} \end{array}\right) \qquad (11)$$

III. PERFORMANCE ANALYSIS

In the previous section the basic model of the system has been presented, and the expression for the instantaneous received SINR of D has been derived. In this section, based on the system model and theoretical analysis in the previous section, the performance of the investigated communication system is further analyzed and the exact closed-form expressions for the OP and channel capacity of the RIS-assisted system with variable transmission distance and simultaneous presence of CCI and phase error are derived.

A. Outage probability analysis

In wireless communication systems, the system outage occurs when the transmission rate of the randomly varying information obtained falls below a certain level. The OP of the system can be defined as the SINR received at the receiver is lower than the given OP threshold, which means the system can be considered to be in an outage condition when $\gamma < \gamma_{th}$, i.e.

$$P_{out} = P_\gamma(\gamma < \gamma_{th}) \qquad (12)$$

Substituting the expression of the PDF of the SINR of user device D as shown in equation (11) into the definition, the expression of the OP of the system can be derived as

$$P_{out} = F_\gamma(\gamma_{th}) = \int_0^{\gamma_{th}} f_\gamma(\gamma)d\gamma \qquad (13)$$

It can be seen from equation (13) that the OP can be further derived from the cumulative distribution function (CDF) of

γ, which can be obtained according to equation (11) [32]. Therefore, the CDF of γ could be obtained as

$$F_\gamma(\gamma) = \int_0^\gamma f_{\gamma_D}(\gamma)d\gamma$$
$$= \int_0^\gamma \frac{\sigma^2 R^\delta}{\delta\bar{\gamma}\Gamma(N)}G_{2,3}^{2,2}\left(\frac{R^\delta\sigma^2\gamma}{2\bar{\gamma}}\ \middle|\ \begin{array}{c} -1, -\frac{2}{\delta} \\ N-1, 0, -1-\frac{2}{\delta} \end{array}\right)d\gamma \qquad (14)$$

Using the properties of the Meijer G function [33], we further reduce equation (14) to

$$F_\gamma(\gamma) = \frac{\sigma^2 R^\delta}{\delta\bar{\gamma}\Gamma(N)}\gamma G_{3,4}^{2,3}\left(\frac{R^\delta\sigma^2\gamma}{2\bar{\gamma}}\ \middle|\ \begin{array}{c} 0, -1, -\frac{2}{\delta} \\ N-1, 0, -1-\frac{2}{\delta}, -1 \end{array}\right) \qquad (15)$$

As can be seen from equation (13), the OP is actually the result of the user's SINR taking a specific value of CDF. Therefore the OP threshold γ_{th} has been taken in equation (15), and the mathematical expression for the OP could be obtained as

$$P_{out} = \frac{\sigma^2 R^\delta}{\delta\bar{\gamma}\Gamma(N)}\gamma_{th}G_{3,4}^{2,3}\left(\frac{R^\delta\sigma^2\gamma_{th}}{2\bar{\gamma}}\ \middle|\ \begin{array}{c} 0, -1, -\frac{2}{\delta} \\ N-1, 0, -1-\frac{2}{\delta}, -1 \end{array}\right) \qquad (16)$$

B. System channel capacity

The channel capacity of the system refers to the maximum amount of information transmitted by the channel in unit time. In an additive Gaussian white noise communication system for continuous channels, according to the Shannon formula, the channel capacity can be expressed as

$$C = B\log_2(1 + \text{SINR}) \qquad (17)$$

where C refers to the channel capacity, B refers to the bandwidth, and SINR indicates the received signal-to-interference-plus-noise ratio.

For the system studied in this paper, the channel obeys a specific distribution and its SINR is a function of the channel random variables, so its Shannon capacity is also a function of the channel random variables. Therefore, the Shannon capacity statistics can be calculated based on the distribution of the random variable function. In this case, the Shannon capacity could be obtained as the mathematical expectation of the equation above

$$C = B\mathbb{E}[\log_2(1 + \text{SINR})] \qquad (18)$$

where $\mathbb{E}[\bullet]$ represents the average expectation.

Without loss of generality, we consider the channel capacity with unit bandwidth, which could also be treated as spectral efficiency. According to equation (18) and referring to the [34] we can obtain the expression for the capacity of the system as equation (19) on the top of the next page.

In order to obtain the closed-form expression, the logarithmic function is firstly represented by the Meijer G function [35], which greatly facilitates the derivation. The relationship between logarithmic function and Meijer G function could be expressed as

$$\ln(1 + x) = G_{2,2}^{1,2}\left(x\ \middle|\ \begin{array}{c} 1, 1 \\ 1, 0 \end{array}\right) \qquad (20)$$

$$f_{\gamma_D}\left(\gamma\right) = \int_0^\infty y f_X\left(y\gamma\right) f_Y(y) dy = \int_0^\infty \frac{yR^\delta}{2\delta\overline{\gamma}\Gamma\left(N\right)} G_{1,3}^{2,1}\left(\frac{R^\delta y\gamma}{4\overline{\gamma}} \;\middle|\; \begin{matrix} -\frac{2}{\delta} \\ N-1, 0, -1-\frac{2}{\delta} \end{matrix}\right) \frac{1}{2\sigma^2} e^{-\frac{y}{2\sigma^2}} dy \qquad (10)$$

$$C = \int_0^\infty \log_2\left(1+x\right) f_\gamma(x) dx = \frac{\sigma^2 R^\delta}{\delta\overline{\gamma}\Gamma\left(N\right)\ln\left(2\right)} \int_0^\infty \ln\left(1+x\right) G_{2,3}^{2,2}\left(\frac{R^\delta\sigma^2 x}{2\overline{\gamma}} \;\middle|\; \begin{matrix} -1, -\frac{2}{\delta} \\ N-1, 0, -1-\frac{2}{\delta} \end{matrix}\right) dx \qquad (19)$$

So we can rewrite (19) as equation (21) on the top of the next page, where procedure (a) is performed using results in [31].

IV. SIMULATION RESULTS AND NUMERICAL ANALYSIS

In this section, we verify the accuracy of the above theoretical derivation using Monte Carlo simulation, setting the number of samples to 10^6, the outage threshold to 10dB. Combining the range of our constructed RIS-assisted wireless communication system model, according to Table 1 [36], if it is not specifically stated, we choose the path loss exponent within the line of sight in the building, setting $\delta = 1.7$. It should be noted that the power value of Gaussian white noise is very small here, $N_0 = 0.01$dB has been taken when performing Monte Carlo simulation.

Fig. 2 plots the CDF curves at $N = 10, 20, 30$ and $\delta = 1.7$, $\sigma^2 = 0.5$, $R = 5$ according to equation (15) as well as Monte Carlo results. It can be seen that the theoretical and simulated values fit relatively well, confirming the accuracy of the previous derivation.

In Fig. 3 and Fig. 4, we plot the curves of the OP varying with the transmitting power and the number of reflecting elements when $\delta = 1.7$, $\sigma^2 = 0.5$, $R = 5$ and $R = 7.5$, respectively. In Fig. 5, we set $N = 20, \delta = 1.7$, and plot the OP curves for $R = 2.5$, $R = 5$, $R = 7.5$. In both Fig. 3 and Fig. 4, three curves are plotted when the number of RIS reflecting elements is 5, 10 and 20. It can be seen from the figures that the Monte Carlo simulation value and the theoretical value basically match, and the two curves fit well. Taking Fig. 3 as an example, when the transmitting power of the BS is higher, the OP value of the system is smaller, which means the outage of the system is less prone to occur, and the OP value decreases as the number of reflecting elements N increases. From the comparison of Fig. 3 and Fig. 4, combined with Fig. 5, we can see that when N takes the same value, the greater the distance R covered by the RIS, the farther the location of the user distribution from the RIS, and the outage will probably occur. Therefore we can conclude that as the transmit power of the base station and the number of RIS reflecting elements increase, the performance of the system would be better. Similarly,, the RIS-assisted communication system is less likely to interrupt when the user device D and the RIS become closer.

Signal propagation in the wireless channel is deteriorated by multiple reflections from obstacle, refraction, interference between ambiguous signal and fading, diffraction, shadowing, etc [36], [37]. Due to the different communication

TABLE 1. PATH LOSS EXPONENT VALUES FOR DIFFERENT ENVIRONMENTS

Environment	Path Loss Exponent
Free space	2
Obstructed in factories	2 to 3
Obstructed in buildings	4 to 6
Urban area cellular radio	2.7 to 3.5
Shadowed urban cellular radio	3 to 5
In building line-of-sight	1.6 to 1.8

environments, the characteristics of the channel also change where the value of the δ reflects the channel fading condition. δ varies according to time and space in the network [38], [39]. In Table 1 [36] the values of the δ for different communication environments has been presented. In Fig. 6, we set $N = 40, \sigma^2 = 0.5, R = 5, \delta = 1.7, 2, 2.3$ considering three different communication environments and acquire the curve of OP with transmit power P. In Fig. 7, we plot OP curves as the function of δ when the transmit power $P = 20$dB and N takes different values. As can be seen from the Fig. 6 and Fig. 7, as the value of δ grows, the path loss exponent increases, which will lead to the higher outage probability of the system. And conversely the smaller the δ, the more stable the system. It can also be seen that when taking the same value of δ, the outage of the system is more like to occur when the number of RIS reflecting elements N and the transmit power P are large. Therefore, we can conclude from Fig. 6 and Fig. 7 that the RIS deployment should consider the RIS deployment communication environment and the different obstacles encountered in the transmission process, and reasonably design the number of RIS in different communication environments to optimize the transmission efficiency and thus improve the transmission performance of the system.

In Fig. 8, we investigate the effect of the variance σ^2 of the CCI on the OP. We set $N = 15, \delta = 1.7, R = 5$. It is clear from Fig. 8 that the smaller the σ^2, the lower the OP curve, which means that the OP value is smaller. Therefore it can be concluded that a communication system needs to reduce interference or improve the immunity of the receiving equipment as much as possible to improve the communication quality.

In Fig. 9 , we investigate the impact on OP when the BS transmit power P is proportional to the variance of CCI. We set $N = 15, \delta = 1.7, R = 5$. As mentioned before, the theoretical results have been derived by omitting the

$$C = \frac{\sigma^2 R^\delta}{\delta \bar{\gamma} \Gamma(N) \ln(2)} \int_0^\infty G_{2,2}^{1,2}\left(x \left| \begin{matrix} 1,1 \\ 1,0 \end{matrix} \right. \right) G_{2,3}^{2,2}\left(\frac{R^\delta \sigma^2 x}{2\bar{\gamma}} \left| \begin{matrix} -1, -\frac{2}{\delta} \\ N-1, 0, -1 - \frac{2}{\delta} \end{matrix} \right. \right) dx$$
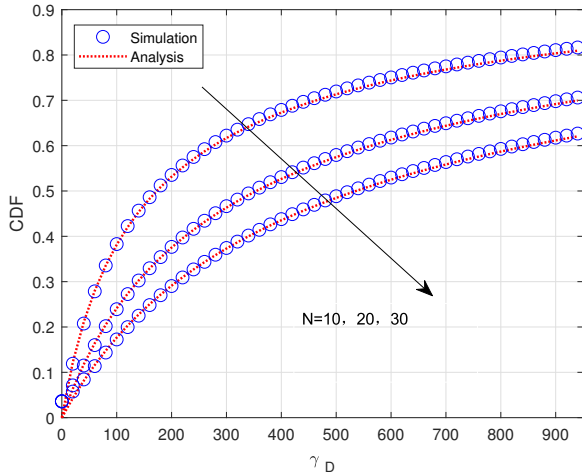$$\overset{(a)}{=} \frac{\sigma^2 R^\delta}{\delta \bar{\gamma} \Gamma(N) \ln(2)} G_{4,5}^{4,3}\left(\frac{R^\delta \sigma^2}{2\bar{\gamma}} \left| \begin{matrix} -1, -1, -\frac{2}{\delta}, 0 \\ -1, -1, N-1, 0, -1 - \frac{2}{\delta} \end{matrix} \right. \right) \tag{21}$$

FIGURE 2. The CDF curve of SINR at D
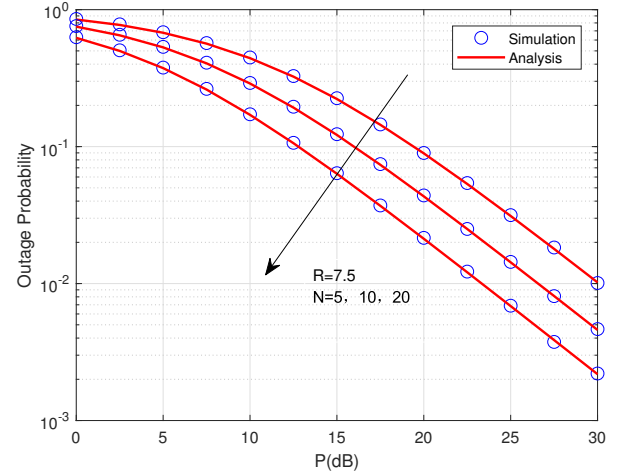
FIGURE 4. Outage probability versus transmit power P when $R = 7.5$, $N = 5, 10, 20$
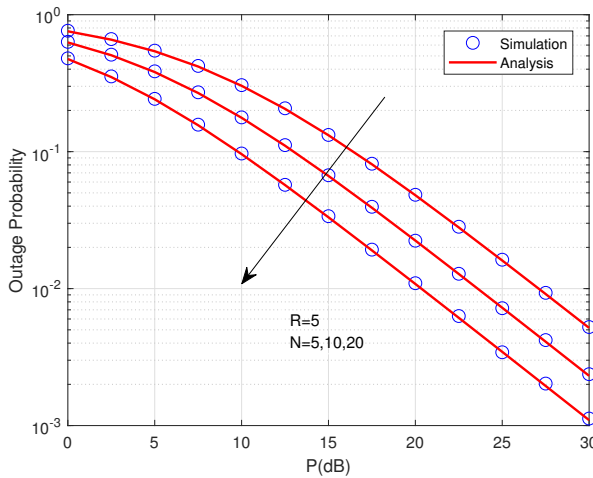
FIGURE 3. Outage probability versus transmit power P when $R = 5$, $N = 5, 10, 20$
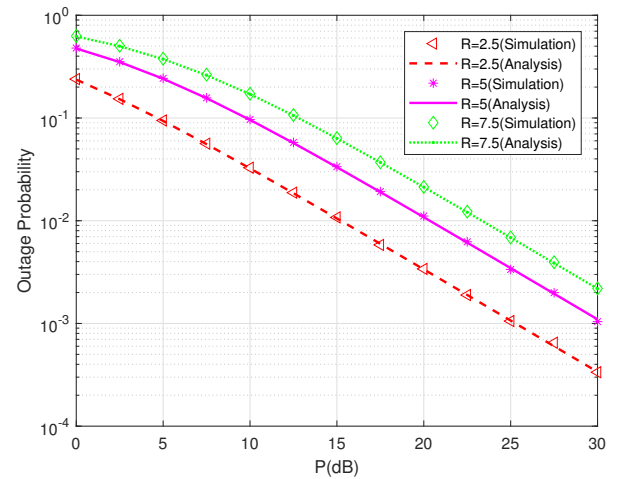

FIGURE 5. Outage probability versus transmit power P when $N = 20$, $R = 2.5, 5, 7.5$

receive noise, while the Monte Carlo simulation is conducted considering the effect of noise on OP in real communication systems. Therefore, the analytical results can be treated as the performance bound in this scenario. Combining equation (3) and the definition of OP, it can be seen from Fig. 9 that the value of the theoretical result is a constant and the system performance increases proportionally with the increase in the proportion of the transmit power P to the variance of the CCI. However, when the BS transmit power

P is low, the OP of the simulated value of the investigated system is very terrible, which is due to the fact that the actual communication system is more affected by noise and the OP value is larger. When the BS transmit power P value gradually increases to -20 dB, the OP of the simulated value rapidly decreases, as P increases to a certain value the simulated value and the theoretical value overlap, which is due to the fact that when P is large enough, the noise
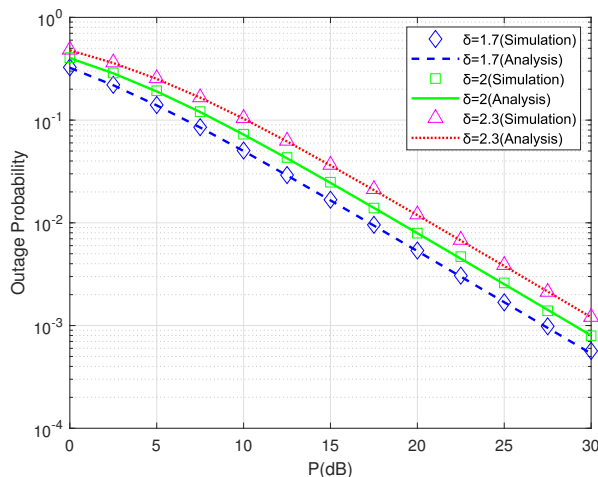
FIGURE 6. Outage probability versus transmit power P when $N = 40, \delta = 1.7, 2, 2.3$
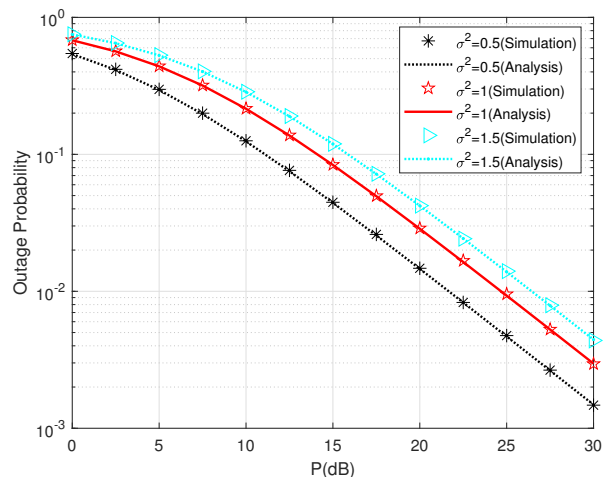

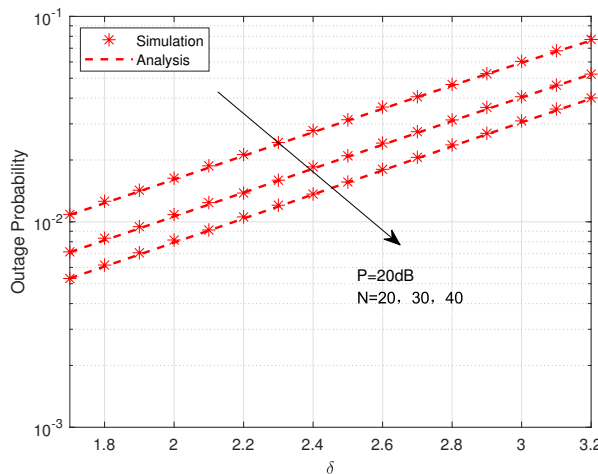**FIGURE 8. Outage probability versus transmit power P when $N = 15, \sigma^2 = 0.5, 1, 1.5$**

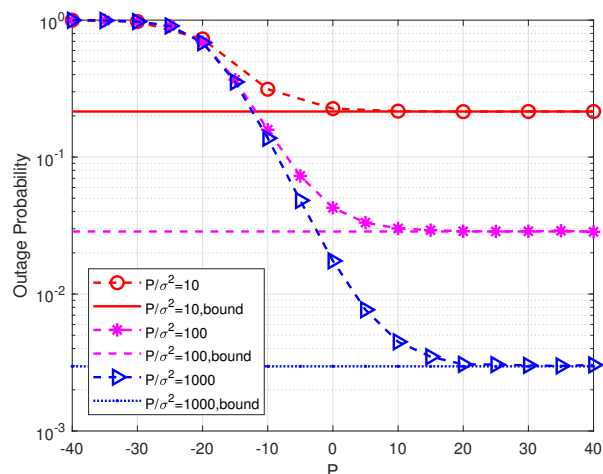**FIGURE 7. Outage probability versus δ when $P = 20$dB, $N = 20, 30, 40$**

FIGURE 9. Outage probability versus transmit power P when $N = 15, P/\sigma^2 = 10, 100, 1000$

has little effect on the actual communication, and the SINR in D is approximated as a constant. As can be seen from Fig. 9, the assumption of omitting noise is reasonable. In the case of known interference, the theoretical results can be used to determine the transmit power of the BS to achieve a specific outage performance. In the case of known interference noise, the theoretical results could been used to determine the transmit power of BS to achieve the specific outage performance.

In Fig. 10, we plot the curve of channel capacity versus the variation with BS transmit power P and the number of RIS reflecting elements N. We set $\delta = 1.7, N = 15, R = 5, 10, 20$. The theoretical and simulated values are very closely fitted. But when the transmit power P is too small, it is practically impossible to achieve. That is, the transmit power from the BS to the user device D

is not sufficient to meet the user's requirements. As the BS transmit power P increases, the slope of the curve becomes progressively larger, and the larger the value of the RIS reflective elements N, the larger the channel capacity. Therefore, we can conclude that the best compromise should be made between the number of RIS reflecting elements and the transmit power P when a communication system meets a given system performance.

In Fig. 11, the impact of the maximum radius of RIS coverage on channel capacity is investigated. We set $N = 15, \delta = 1.7, \sigma^2 = 0.5$, study the variation of channel capacity with R. As can be seen in Fig. 11 the magnitude of the channel capacity is inversely proportional to R. Moreover, as the maximum radius value increases, the channel capacity value decreases accordingly, and the system performance
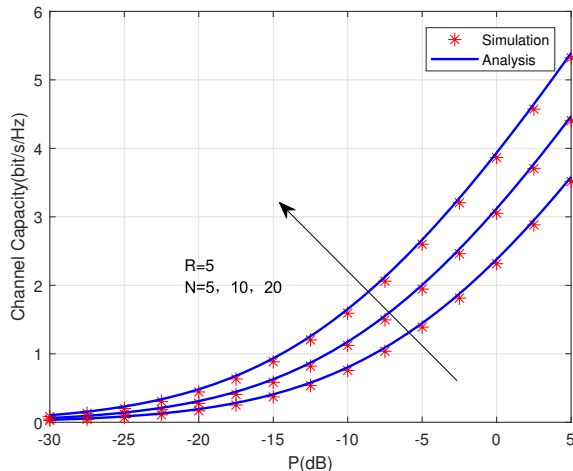
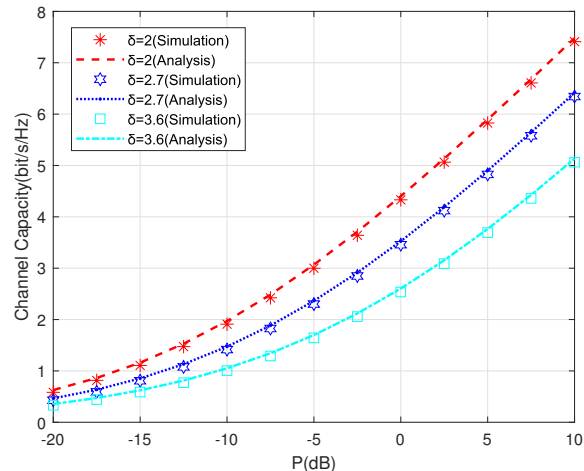**FIGURE 10. Channel capacity versus transmit power P when $N = 5, 10, 20$**

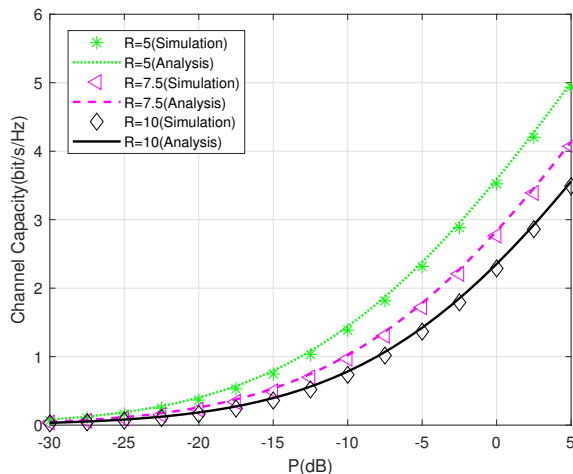**FIGURE 12. Channel capacity versus transmit power P when $N = 40, \delta = 2, 2.7, 3.6$**

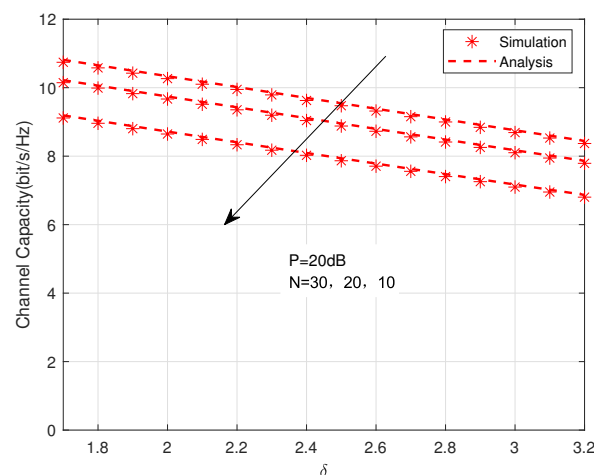**FIGURE 11. Channel capacity versus transmit power P when $N = 15, R = 5, 7.5, 10$**

FIGURE 13. Channel capacity versus δ when $P = 20$dB, $N = 10, 20, 30$

decreases by 17.4% for $R = 7.5$ and 29.2% for $R = 10$ compared with $P = 5$dB and $R = 5$. The reason for this is that as the distance R increases, the power of the reflected signal received by the user device D from the RIS decreases, the interference becomes greater, and the system performance decreases. On the contrary, the closer the distance between user D and RIS, the stronger the reflected signal received from RIS and the better the communication quality. Consequently, in the actual deployment of RIS, the communication distance between RIS and users should be reasonably considered.

In analogy to the analysis of the OP, we consider the channel capacity in three different mobile wireless communication environments and also analyze the variation of channel capacity with δ. In Fig. 12 we set $N = 40, R =$

$5, \sigma^2 = 0.5, \delta = 2, 2.7, 3.6$ and in Fig. 13 we set $P = 20$dB, $R = 5, \sigma^2 = 0.5, N = 10, 20, 30$. It can be seen from Fig. 13 that the path loss exponent δ and the channel capacity are inversely proportional. Combining Fig. 12 and 13, it is evident that when the value of δ increases, the system performance decreases. This is because the larger value of δ, the propagation conditions are poorer.

The effect of the variance σ^2 of CCI on the channel capacity has been shown in Fig. 14, where $\delta = 1.7, N = 15, R = 5$ and three different values of σ^2 has been considered. As can be seen from Fig. 14 the smaller the value of σ^2, the greater the channel capacity of the system, and the smaller the variance σ^2, the tighter the fit of the curve. Therefore, it could conclude that, the smaller the value of the CCI , the larger the channel capacity.
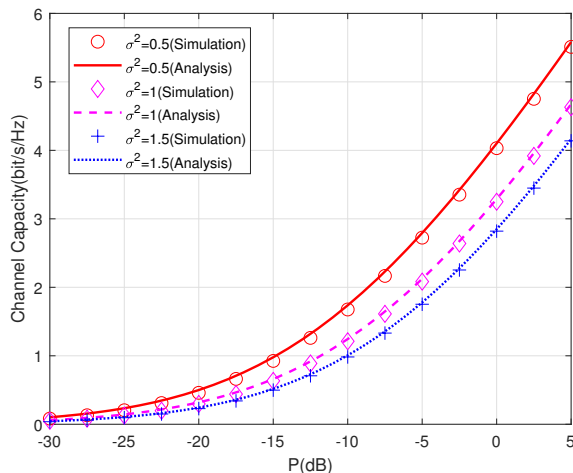
FIGURE 14. Channel capacity versus transmit power P when $N = 15, \sigma^2 = 0.5, 1, 1.5$
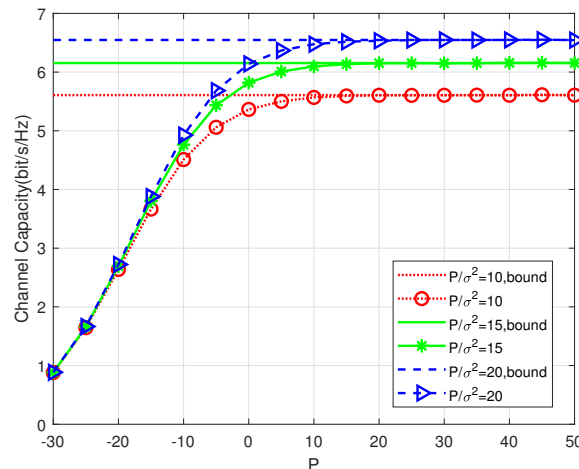

FIGURE 15. Channel capacity versus transmit power P when $N = 15, P/\sigma^2 = 10, 15, 20$

In Fig. 15, we set $\delta = 1.7, N = 15, R = 5$. In analogy to the analysis of the OP, we investigate the implications on system channel capacity when the BS transmit power and the variance of the CCI are proportional. The analytical results have been plotted as the bound of the practical performance. From the Fig. 15, it can be seen that when the transmit power is extremely low, the simulation results is deviated from performance bound due to the influence of the noise. When the transmit power gradually increases large enough, the effect of the CCI on the system is greater than that of Gaussian noise. The SINR at D tends to be a constant at this time, and the channel capacity is also nearly a constant due to its relationship with the SINR of the system. From this it can be concluded that in the scenario where the receive noise could not been omitted, the derived analytical results could also been considered as a effective performance bound of the system.

V. CONCLUSION

This paper focuses on the performance of RIS-assisted wireless communication systems with CCI. Firstly, closed-form expressions for OP and channel capacity are derived. Secondly, the effect of various factors on the OP and capacity of the system is further analyzed. Finally the accuracy of the theoretical derivation is verified using Monte Carlo simulation. The system model proposed in this paper takes into account the existence of phase error and user location uncertainty, which is more in line with the actual situation, and the conclusions obtained can provide some theoretical basis for the actual deployment of RIS. Simulation results present the relationship between system parameters and system performance. Furthermore, CCI also has an impact on system performance and it is necessary to minimize interference in the vicinity of the user to further improve the performance of the system. Besides, the value of the

BS transmit power should be designed reasonably since the transmit power could be transformed as CCI for other user devices. In the future, the trade-off between transmit power and CCI in the view of the communication network could be further investigated.

REFERENCES

[1] J. Zhang, E. Björnson, M. Matthaiou, D. W. K. Ng, H. Yang, and D. J. Love, "Prospective multiple antenna technologies for beyond 5G," *IEEE Journal on Selected Areas in Communications*, vol. 38, no. 8, pp. 1637–1660, 2020.

[2] J. Wang, W. Zhang, X. Bao, T. Song, and C. Pan, "Outage analysis for intelligent reflecting surface assisted vehicular communication networks," in *GLOBECOM 2020-2020 IEEE Global Communications Conference*. IEEE, 2020, pp. 1–6.

[3] Q. Wu and R. Zhang, "Intelligent reflecting surface enhanced wireless network via joint active and passive beamforming," *IEEE Transactions on Wireless Communications*, vol. 18, no. 11, pp. 5394–5409, 2019.

[4] G. C. Alexandropoulos, K. Stylianopoulos, C. Huang, C. Yuen, M. Bennis, and M. Debbah, "Pervasive machine learning for smart radio environments enabled by reconfigurable intelligent surfaces," *Proceedings of the IEEE*, vol. 110, no. 9, pp. 1494–1525, 2022.

[5] Z. Xie, W. Yi, X. Wu, Y. Liu, and A. Nallanathan, "Downlink multi-RIS aided transmission in backhaul limited networks," *IEEE Wireless Communications Letters*, vol. 11, no. 7, pp. 1458–1462, 2022.

[6] H. Dai, W. Huang, H. Zhang, J. Luo, C. Li, and B. Wang, "Achievable harvested energy region of IRS-assisted wireless power transfer system," in *2021 13th International Conference on Wireless Communications and Signal Processing (WCSP)*. IEEE, 2021, pp. 1–5.

[7] K. Song, J. Zhang, Z. Ji, J. Jiang, and C. Li, "Energy-efficiency for IoT system with cache-enabled fixed-wing UAV relay," *IEEE Access*, vol. 8, pp. 117 503–117 512, 2020.

[8] R. A. Tasci, F. Kilinc, E. Basar, and G. C. Alexandropoulos, "A new RIS architecture with a single power amplifier: Energy efficiency and error performance analysis," *IEEE Access*, vol. 10, pp. 44 804–44 815, 2022.

[9] L. Yang, F. Meng, Q. Wu, D. B. da Costa, and M.-S. Alouini, "Accurate closed-form approximations to channel distributions of RIS-aided wireless systems," *IEEE Wireless Communications Letters*, vol. 9, no. 11, pp. 1985–1989, 2020.

[10] D. Selimis, K. P. Peppas, G. C. Alexandropoulos, and F. I. Lazarakis, "On the performance analysis of RIS-empowered communications over Nakagami-m fading," *IEEE Communications Letters*, vol. 25, no. 7, pp. 2191–2195, 2021.

This article has been accepted for publication in IEEE Open Journal of the Communications Society. This is the author's version which has not been fully edited and content may change prior to final publication. Citation information: DOI 10.1109/OJCOMS.2023.3244648

Bian *et al.*: Performance Analysis of RIS-Assisted Wireless Communication Systems under Co-Channel Interference

[11] X. Cao, B. Yang, H. Zhang, L. Qian, C. Yuen, and Z. Han, "Reconfigurable intelligent surface assisted internet-of-things: MAC design and optimization," in *2021 IEEE Wireless Communications and Networking Conference Workshops (WCNCW)*, 2021, pp. 1–6.

[12] I. Trigui, W. Ajib, and W.-P. Zhu, "Secrecy outage probability and average rate of RIS-aided communications using quantized phases," *IEEE Communications Letters*, vol. 25, no. 6, pp. 1820–1824, 2021.

[13] Y. Zhang, J. Zhang, M. D. Renzo, H. Xiao, and B. Ai, "Performance analysis of RIS-aided systems with practical phase shift and amplitude response," *IEEE Transactions on Vehicular Technology*, vol. 70, no. 5, pp. 4501–4511, 2021.

[14] A. Faisal, I. Al-Nahhal, O. A. Dobre, and T. M. N. Ngatched, "Deep reinforcement learning for RIS-assisted FD systems: Single or distributed RIS?" *IEEE Communications Letters*, vol. 26, no. 7, pp. 1563–1567, 2022.

[15] H. Zhang, B. Di, L. Song, and Z. Han, "Reconfigurable intelligent surfaces assisted communications with limited phase shifts: How many phase shifts are enough?" *IEEE Transactions on Vehicular Technology*, vol. 69, no. 4, pp. 4498–4502, 2020.

[16] S. Zeng, H. Zhang, B. Di, Z. Han, and L. Song, "Reconfigurable intelligent surface (RIS) assisted wireless coverage extension: RIS orientation and location optimization," *IEEE Communications Letters*, vol. 25, no. 1, pp. 269–273, 2021.

[17] M. H. Dinan, N. S. Perović, and M. F. Flanagan, "RIS-assisted receive quadrature space-shift keying: A new paradigm and performance analysis," *IEEE Transactions on Communications*, vol. 70, no. 10, pp. 6874–6889, 2022.

[18] Y. Han, S. Zhang, L. Duan, and R. Zhang, "Cooperative double-IRS aided communication: Beamforming design and power scaling," *IEEE Wireless Communications Letters*, vol. 9, no. 8, pp. 1206–1210, 2020.

[19] Z. Xie, W. Yi, X. Wu, Y. Liu, and A. Nallanathan, "Downlink multi-RIS aided transmission in backhaul limited networks," *IEEE Wireless Communications Letters*, vol. 11, no. 7, pp. 1458–1462, 2022.

[20] H. Zhang, L. Song, Z. Han, and H. V. Poor, "Spatial equalization before reception: Reconfigurable intelligent surfaces for multi-path mitigation," in *ICASSP 2021 - 2021 IEEE International Conference on Acoustics, Speech and Signal Processing (ICASSP)*, 2021, pp. 8062–8066.

[21] C. Zhong, S. Jin, and K.-K. Wong, "Dual-hop systems with noisy relay and interference-limited destination," *IEEE Transactions on Communications*, vol. 58, no. 3, pp. 764–768, 2010.

[22] A. Shah and A. Haimovich, "Performance analysis of optimum combining in wireless communications with rayleigh fading and cochannel interference," *IEEE Transactions on Communications*, vol. 46, no. 4, pp. 473–479, 1998.

[23] N. Cherif, I. Trigui, and S. Affes, "On the performance analysis of mixed multi-aperture FSO/multiuser RF relay systems with interference," in *2017 IEEE 18th International Workshop on Signal Processing Advances in Wireless Communications (SPAWC)*, 2017, pp. 1–5.

[24] A. Sikri, A. Mathur, P. Saxena, M. R. Bhatnagar, and G. Kaddoum, "Reconfigurable intelligent surface for mixed FSO-RF systems with co-channel interference," *IEEE Communications Letters*, vol. 25, no. 5, pp. 1605–1609, 2021.

[25] L. Yang, P. Li, Y. Yang, S. Li, I. Trigui, and R. Ma, "Performance analysis of RIS-aided networks with co-channel interference," *IEEE Communications Letters*, vol. 26, no. 1, pp. 49–53, 2022.

[26] A. Bansal, N. Agrawal, and K. Singh, "Rate-splitting multiple access for UAV-based RIS-enabled interference-limited vehicular communication system," *IEEE Transactions on Intelligent Vehicles*, pp. 1–1, 2022.

[27] S. Li, J. Zhao, W. Tan, and C. You, "Optimal secure transmit design for wireless information and power transfer in V2X vehicular communication systems," *AEU-International Journal of Electronics and Communications*, vol. 118, p. 153148, 2020.

[28] W. Zhang, X. Xia, Y. Fu, and X. Bao, "Hybrid and full-digital beamforming in mmWave massive MIMO systems: A comparison considering low-resolution ADCs," *China Communications*, vol. 16, no. 6, pp. 91–102, 2019.

[29] K. Song, B. Ji, Y. Huang, M. Xiao, and L. Yang, "Performance analysis of heterogeneous networks with interference cancellation," *IEEE Transactions on Vehicular Technology*, vol. 66, no. 8, pp. 6969–6981, 2017.

[30] L. Kong, S. Kisseleff, S. Chatzinotas, B. Ottersten, and M. Erol-Kantarci, "Effective rate of RIS-aided networks with location and phase estimation uncertainty," in *2022 IEEE Wireless Communications and Networking Conference (WCNC)*, 2022, pp. 2071–2075.

[31] I. S. Gradshteyn and I. M. Ryzhik, *Table of integrals, series, and products*. Academic press, 2014.

[32] V. M. Kapinas, S. K. Mihos, and G. K. Karagiannidis, "On the monotonicity of the generalized Marcum and Nuttall *Q*-functions," *IEEE Transactions on Information Theory*, vol. 55, no. 8, pp. 3701–3710, 2009.

[33] A. P. Prudnikov, J. A. Bryčkov, and O. I. Maričev, *Integrals and series. Vol. 3, More special functions*. Gordon and Breach, 2003.

[34] A. Makarfi, K. Rabie, O. Kaiwartya, O. Badarneh, G. Nauryzbayev, and R. Kharel, "Physical layer security in RIS-assisted networks in Fisher-Snedecor composite fading," in *2020 12th International Symposium on Communication Systems, Networks and Digital Signal Processing (CSNDSP)*, 2020, pp. 1–6.

[35] V. S. Adamchik and O. I. Marichev, "The algorithm for calculating integrals of hypergeometric type functions and its realization in reduce system," in *International Symposium on Symbolic and Algebraic Computation*, 1990.

[36] V. Dharmadhikari, N. Pusalkar, and P. Ghare, "Path loss exponent estimation for wireless sensor node positioning: Practical approach," in *2018 IEEE International Conference on Advanced Networks and Telecommunications Systems (ANTS)*, 2018, pp. 1–4.

[37] C. C. Pu, P. C. Ooi, B. G. Lee, and W.-Y. Chung, "Analysis of path loss exponent error in ranging and localization of wireless sensor network," in *International Conference on Frontiers of Communications, Networks and Applications (ICFCNA 2014 - Malaysia)*, 2014, pp. 1–6.

[38] D. Li and J. Huang, "RSS based method for sensor localization with unknown transmit power and uncertainty in path loss exponent," in *2016 8th IEEE International Conference on Communication Software and Networks (ICCSN)*, 2016, pp. 298–302.

[39] V. Dharmadhikari, N. Pusalkar, and P. Ghare, "Path loss exponent estimation for wireless sensor node positioning: Practical approach," in *2018 IEEE International Conference on Advanced Networks and Telecommunications Systems (ANTS)*, 2018, pp. 1–4.

YUYING BIAN is pursuing her B.S. degree in Qingdao University. Her current research interests include reconfigurable intelligent surface, wireless communication and signal processing.

DANDAN DONG received her B.S. degree in telecommunication engineering from Qingdao University, Qingdao, China in 2020. She is pursuing her M.S. degree in Qingdao University. Her current research interests include reconfigurable intelligent surface, cooperative communication.

JING JIANG (Member, IEEE) received the M.Sc. degree from Xi Dian University, in 2005, and the Ph.D. degree in information and communication engineering from North Western Polytechnic University, China, in 2009. She was the leader of 3GPP LTE MIMO project with ZTE Corporation, China, from 2006 to 2013. Currently, she is a Professor with the Shaanxi Key Laboratory of Information Communication Network and Security, Xi'an University of Posts and Telecommunications, Xi'an, China. Her research interests include

massive multiple-input multiple-output systems and millimeter-wave communications. She has been a member of 3GPP.

KANG SONG (Member, IEEE) received the B.S. degree from Anhui University, China in 2009. In 2016 he received the Ph.D. degree in information and communication engineering from Southeast University, China. Since August 2016, he has been a faculty in the School of Electronic and Information Engineering, Qingdao University. His current research interests include RIS-assisted cooperative communications and intelligent signal processing.